

*The Fast Wavelet Transform and its Application to
Electroencephalography:*

A Study of Schizophrenia

Prepared by:

Cullen Jon Navarre Roth

May 7, 2014

ACKNOWLEDGMENTS

I would like to thank the National Science Foundation for its support through the Fall of the academic year of 2014 “Mentoring through Critical Transition Points” (MCTP) grant DMS 1148001. I would also like to thank the Undergraduate Committee, especially Professor Monika Nitsche in her dual role as Chair of the Undergraduate Committee and PI of the MCPT grant. I would also like to thank Professor Christina Pereyra, Dr. David Bridwell, Dr. NavinCota Gupta, Dr. Vince Calhoun, and Dr. Maggie Werner-Washburne for their support and encouragement.

TABLE OF CONTENTS

Table of Contents

Chapter 1	Introduction	1
Chapter 2	Preliminaries	2
2.1.	The Wavelet Basis	2
2.2.	Orthogonal Multiresolution Analysis (MRA):	3
Chapter 3	Scaling Equation and Conjugate Mirror Conditions	8
3.1.	The Scaling Equation	8
3.2.	Conjugate Mirror Filters	11
3.3.	The Wavelet and Conjugate Mirror Filters.....	13
Chapter 4	Biorthogonality and its Implication	16
4.1.	Biorthogonal MRA	16
4.2.	Biorthogonal Scaling equations	20
4.3.	Finite Impulse Response Filters and Fast Wavelet Transform.....	21
Chapter 5	Wavelets and Electroencephalography	23
5.1.	Background on Schizophrenia	23
5.2.	Materials and Methods.....	23
5.3.	Results	24
5.4.	Conclusions and Closing Remarks	28
Appendix	33
Bibliography	35

Chapter 1 Introduction

Unveiling the transient world is a complex and compelling problem in applied mathematics. Numerous technologies and analytics have been created to study dynamic signals. The wavelet transform is one such tool. The wavelet transform grants us the ability to deconstruct multifaceted signals into time frequency representations which allows the user to zoom into and take apart an observed signal.

The deconstruction ability of the wavelet transform is generated by multiresolution properties. Not only do these unique properties produce time series information regarding a signal but they also grant frequency information. With each level of deconstruction of a signal, we may observe different contributing waveforms to the signal in certain frequency bandwidths or intervals.

While the wavelet transform is unique, its applications are many. An area of application and the focus of this study is signal processing. Specifically the processing and analysis of electrical potentials generated from the scalp or more commonly named electroencephalographic (EEG) responses.

These signals are of interest because they are related to brain health and cognition. Individuals diagnosed with schizophrenia demonstrate a reduced event related potential (ERP) ~300 ms after the presentation of a rare stimulus [24]. This response is associated with the reorganization toward unexpected events.

This study will explore the time-frequency characteristics of these responses using wavelet analysis and examine the degree in which responses are modulated by regularities in the environment within healthy individuals and individuals diagnosed with schizophrenia.

Chapter 2 Preliminaries

2.1. The Wavelet Basis

A function $\psi \in L^2(\mathbb{R})$ is a wavelet if $\{\psi_{j,k} := 2^{-j/2} \psi(2^{-j}t - k) \text{ for } j, k \in \mathbb{Z}\}$ forms an orthonormal basis for $L^2(\mathbb{R})$. This basis is called a wavelet basis. The wavelet transform involves the use of translations and scaling instead of modulations. This provides the wavelet transform with a natural zooming mechanic. We will talk more about this zooming mechanism in the Orthogonal Multiresolution section. With a wavelet transform the idea is to deconstruct a signal into an approximation and a set of details.

Definition 1. The orthogonal wavelet transform is defined as the function that maps $L^2(\mathbb{R})$ the set of $L^2(\mathbb{R})$ itegrable functions to the *little l^2 of the Integers*, over the complex numbers, and assigns each function in $L^2(\mathbb{R})$ a sequence of wavelet coefficients:

$$W_j f(j, k) := \langle f, \psi_{j,k} \rangle = \int_{\mathbb{R}} f(x) \overline{\psi_{j,k}(x)} dx \quad (1)$$

2.2. Orthogonal Multiresolution Analysis (MRA):

Definition 2. [13], [7] A multiresolution analysis (MRA) is a decomposition of $L^2(\mathbb{R})$ the set of square integrable functions on \mathbb{R} into a set of nested subspaces where V_0 is the central space. An MRA satisfies the following properties:

$$\forall j \in \mathbb{Z}, \quad V_{j+1} \subset V_j \quad (2)$$

$$\forall j \in \mathbb{Z}, f(t) \in V_j \Leftrightarrow f\left(\frac{t}{2}\right) \in V_{j+1} \quad (3)$$

$$\lim_{j \rightarrow +\infty} V_j = \bigcap_{j=-\infty}^{+\infty} V_j = \{0\} \quad (4)$$

$$\lim_{j \rightarrow -\infty} V_j = \text{closure} \left(\bigcup_{j=-\infty}^{j=+\infty} V_j \right) = L^2(R) \quad (5)$$

The integer translates of the scaling function φ form an orthonormal basis for V_0 (6)

Definition 3. [Meyer] The scaling function mentioned in (6) we will define:

$$\varphi_{j,k}(t) := 2^{-\frac{j}{2}} \varphi(2^{-j} t - k) \quad (7)$$

Theorem 4. ([13], Theorem 7.1) Let $\{V_j\}_{j \in \mathbb{Z}}$ be an MRA with a scaling function φ whose dilations and translations according to (6) form an orthonormal basis of V_0 . Then the family $\{\varphi_{j,k}\}_{k \in \mathbb{Z}}$ is also an orthonormal basis of $\{V_j\}_{j \in \mathbb{Z}}$.

Briefly we will discuss the MRA and its properties. Property (2) states that the subspaces are nested. Each space expresses a level of detail that is contained in the subspace above.

$$\dots V_3 \subset V_2 \subset V_1 \subset V_0 \subset V_{-1} \subset V_{-2} \subset V_{-3} \dots$$

Here it is important to note that depending on the author the index of the subspaces may be different; for example, Matlab© software, [13],[7] has an increasing index with declining subspaces. In other words:

$$\lim_{j \rightarrow -\infty} V_j = L^2(R).$$

The scaling function allows us to climb upward and downward from space to space. This is seen in the scaling property (3). This property along with (6) allows us to calculate any detail in space at a resolution 2^{j+1} using only the

information from the space above at a resolution 2^j . As the resolution gets worse ($j \rightarrow \infty$) (4) implies that we will eventually lose all detail. Thus we can see that the scaling function, φ completely defines its MRA.

There is also a sequence of related orthogonal subspaces W_j of $L^2(R)$ that are related to our V_j . While not completely necessary, in an *orthogonal* MRA we require that $V_j \perp W_j$ for all j ([7], [14]). These spaces are then connected in an MRA by

$$V_j = V_{j+1} \oplus W_{j+1}$$

Here we are using the “Matlab” indexing, where the space $V_{j+1} \subset V_j$. The \oplus symbol is the summation of the orthogonal spaces W_j of $L^2(R)$.

When decomposing a signal, we start with the finest or “best” approximation for the signal and choose the lowest level of detail for decomposition. So we will have spaces nested:

$$V_n \subset \dots V_3 \subset V_2 \subset V_1 \subset V_0$$

such that we can use the \oplus symbol and truncate the information to attain:

$$V_0 = V_n \oplus \sum_{j=1}^n W_j$$

Example 5. For the central space V_0 when decomposed to 3 levels, we may represent the central space as

$$V_0 = V_1 \oplus W_1$$

$$V_0 = V_2 \oplus W_2 \oplus W_1$$

$$V_0 = V_3 \oplus W_3 \oplus W_2 \oplus W_1$$

In neurology the convention is to denote the spaces $\{W_3, W_2, W_1\}$ as *octaves* and the space V_3 as the *residual* space ([1],[2],[3],[4],[5]).

□

Theorem 6. [17](Mallat's Theorem) Given an orthogonal MRA with scaling function φ , there is a wavelet $\psi \in L^2(\mathbb{R})$ such that for each $j \in \mathbb{Z}$, the family $\{\psi_{j,k}\}_{k \in \mathbb{Z}}$ is an orthonormal basis for W_j . Hence the family $\{\psi_{j,k}\}_{k \in \mathbb{Z}}$ is an orthonormal basis for $L^2(\mathbb{R})$.

From Theorem 6 (Mallat's Theorem), a central and basic tenant in multiresolution analysis, ([7]) whenever we have an MRA that satisfies (2) – (6) we have a family of wavelet functions defined as (from [Meyer])

$$\psi_{j,k} := 2^{-\frac{j}{2}} \psi_{j,k}(2^{-j}t - k) \quad j, k \in \mathbb{Z} \quad (8)$$

Theorem 6 states that (8) exists, is determined by the scaling function φ , and forms an orthonormal wavelet basis for W_j . The W_j spaces in an orthogonal MRA are referred to as the wavelet spaces or *detail* spaces. A proof of Theorem 6 may be found in [17], [14], [13], and [7].

Returning to the definition of an MRA, it follows that the fifth property (5) of an *orthogonal* MRA may be restated as:

$$L^2(\mathbb{R}) = \overline{\bigoplus_{j \in \mathbb{Z}} W_j} \quad (9)$$

Where we have:

$$W_j = \overline{\text{span}\{\psi_{j,k}\}_{k \in \mathbb{Z}}} \quad (10)$$

Definition 7. For a signal (or function) $f(t)$ we will define the orthogonal projection of our signal onto the space V_j as

$$P_j f(t) = \sum_{k \in \mathbb{Z}} \langle f, \varphi_{j,k} \rangle \varphi_{j,k}(t) \quad (11)$$

where $\langle f, \varphi_{j,k} \rangle$ is the inner product of our signal and scaling function (for a definition of the inner product please refer to the appendix, Definition 2A and Definition 3A).

Since $P_j f(t)$ is the orthogonal projection of our signal, it is the “best” approximation of our signal in V_j (see figure 1). From [13], as a consequence of (4), we see that

$$\lim_{j \rightarrow +\infty} \|P_j f\|_2 = 0$$

Then for $P_{j+1} f(t) \in V_{j+1} \subset V_j$ the orthogonal projection $P_j f(t)$ will be a better approximation for our $f(t)$ than $P_{j+1} f(t)$ since by our definition (2) V_{j+1} is nested in V_j .

The difference between our two approximations, $P_j f(t)$ and $P_{j+1} f(t)$ is the orthogonal projection of our signal $f(t)$ onto the orthogonal wavelet space W_{j+1} and can then be calculated

$$Q_{j+1} f(t) = P_j f(t) - P_{j+1} f(t) = \sum_{k \in \mathbb{Z}} \langle f, \psi_{j+1,k} \rangle \psi_{j+1,k}(t) \quad (12)$$

Rewriting equation (12) and inserting equation (11) we obtain:

$$\begin{aligned} P_j f(t) &= P_{j+1} f(t) + Q_{j+1} f(t) \\ P_j f(t) &= \sum_{k \in \mathbb{Z}} \langle f, \varphi_{j+1,k} \rangle \varphi_{j+1,k}(t) + \sum_{k \in \mathbb{Z}} \langle f, \psi_{j+1,k} \rangle \psi_{j+1,k}(t) \end{aligned} \quad (13)$$

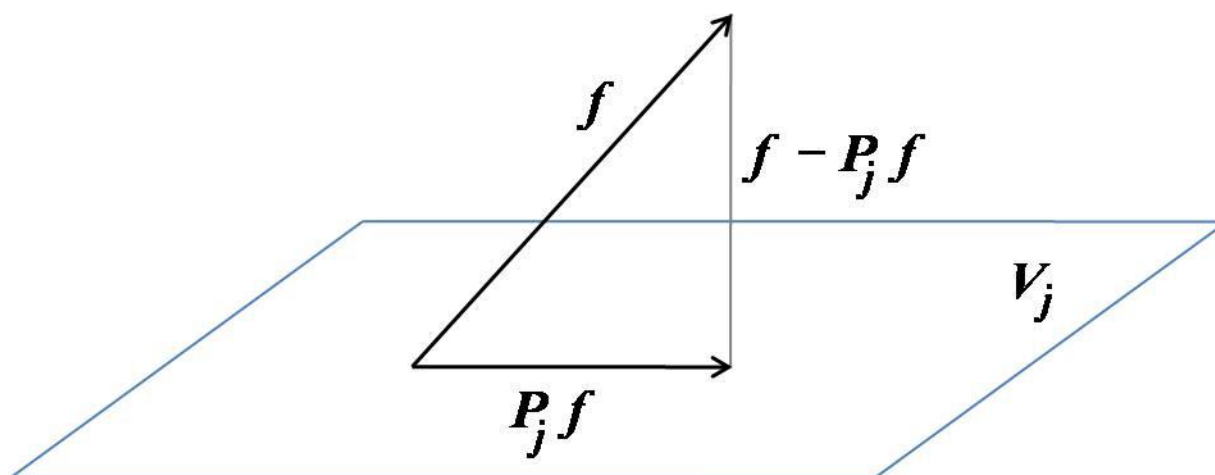


Figure 1 $P_j f$ is the projection of f in the space V_j

Chapter 3 Scaling Equation and Conjugate Mirror Conditions

“The multiresolution theory of orthogonal wavelets proves that any conjugate mirror filter characterizes a wavelet ψ that generates an orthonormal basis of $L^2(\mathbb{R})$.”

S. Mallat

In this chapter, we will discuss the connection between an MRA and scaling equations. This will then lead us to defining conjugate mirror filters.

3.1. The Scaling Equation

Remark 8. Recall (2) – (6) from our MRA because $\varphi \in V_0 \subset V_{-1}$ we may express φ as a superposition of $\varphi_{-1,k}$ where $\varphi_{-1,k}(t)$ forms an orthonormal basis of V_{-1}

$$\varphi_{-1,k}(t) = \sqrt{2}\varphi(2t - k), k \in \mathbb{Z} \quad (14)$$

Meaning, there exists a sequence of coefficients $\{h_k\}_{k \in \mathbb{Z}}$ that satisfy the following scaling equation.

$$\varphi(t) = \sum_{k \in \mathbb{Z}} h_k \varphi_{-1,k}(t) = \sqrt{2} \sum_{k \in \mathbb{Z}} h_k \varphi(2t - k) \quad (15)$$

The sequence of coefficients $\{h_k\}_{k \in \mathbb{Z}}$ are given by the inner product

$$h_k := \langle \varphi, \varphi_{-1,k} \rangle \quad (16)$$

These coefficients $\{h_k\}_{k \in \mathbb{Z}}$ are the so called *low pass filter*. They are often produced from a trigonometric polynomial (such as a *spline* function discussed

CHAPTER 3 SCALING EQUATION AND CONJUGATE MIRROR CONDITIONS

later) with a period of one and with only a few of the coefficients not equal to zero. Thus they are referred to as *finite impulse response filters* (FIR) [13], [7]. We will discuss FIR later in subsequent chapters.

From (16) the sequence of coefficients $\{h_k\}_{k \in \mathbb{Z}}$ can be represented by its refinement mask [13]. This refinement mask is given as:

$$H(\zeta) = \frac{1}{\sqrt{2}} \sum_{k \in \mathbb{Z}} h_k e^{-2\pi i k \zeta} \quad (17)$$

Remark 9. Notice with “z” notation where $z = e^{-2\pi i \zeta}$ (17) is a trigonometric polynomial where (16) is the FIR. (17) is then represented as

$$H(z) = \frac{1}{\sqrt{2}} \sum_{k \in \mathbb{Z}} h_k z^k \quad (18)$$

Theorem 10. ([13], Theorem 7.2) Let $\varphi_{j,k} \in L^2(\mathbb{R})$ be an integrable scaling function (such as 15). The Fourier series of $\{h_k\}_{k \in \mathbb{Z}}$ satisfies

$$|H(\zeta)|^2 + |H(\zeta + 1/2)|^2 = 1 \quad (19)$$

(19) is referred to as a *conjugate mirror filter* condition [13] and is a consequence of the orthonormality of the scaling function which is shown in [14], [7]. For more information and proof of Theorem 10 please refer to ([13], Theorem 7.2). The main result from Theorem 10 is that (19) is a necessary condition to devise (15). Simply the filters determine several properties of the scaling function.

On the Fourier side of equation (15) we see that

CHAPTER 3 SCALING EQUATION AND CONJUGATE MIRROR
CONDITIONS

$$\hat{\varphi}(z) = H(z/2)\hat{\varphi}(z/2) \quad (20)$$

It can be shown [14], [Meyer] that (20) satisfies (19). An alternative condition for the scaling function is shown below [13].

Lemma 11. [13], ([17]. **Lemma 10.75**) Given a function $f \in L(R)^2$ then the family

$\{f_{0,k} = \tau_k f\}_{k \in Z}$ of integer translates of f is orthonormal if and only if

$$\sum_{n \in Z} |\hat{f}(z + n)|^2 = 1 \quad (21)$$

where $\tau_k f(x) := f(x - k)$ for $k \in Z$.

Proof 12. (inspired by [17]). First we will take the inner product between $\tau_k f$ and $\tau_m f$ with k and m elements of the integers. It follows using a change of variables with the definition of inner product we have

$$\langle \tau_k f, \tau_m f \rangle = \langle \tau_{k-m} f, f \rangle$$

For the family of f we may equate their orthonormality via

$$\langle \tau_k f, \tau_m f \rangle = \langle \tau_{k-m} f, f \rangle = \langle \tau_K f, f \rangle = \delta_K \text{ for } K = k - m, \in Z$$

Then we will take the Fourier transform on each side of the equation. We know that the Fourier transform will preserve the inner product [17, exercise 7.32]. From the time frequency dictionary the Fourier transform of $\tau_K f$ will translate to a modulation by $e^{-2\pi i k z}$ a function whose period is one.

$$\delta_K = \langle \widehat{\tau_K f}, \hat{f} \rangle = \int_R e^{-2\pi i k z} |\hat{f}(z)|^2 dz$$

Then we may use the additive property of the integral to sum the integral over the integers. It follows,

CHAPTER 3 SCALING EQUATION AND CONJUGATE MIRROR CONDITIONS

$$\delta_K = \sum_{n \in \mathbb{Z}} \int_n^{n+1} e^{-2\pi i k \zeta} |\hat{f}(\zeta)|^2 d\zeta$$

Next, we will use a change of variables to map the interval $[n, n+1)$ onto a unit interval of $[0, 1)$ by setting $m = \zeta - n$. Thus the equation above becomes

$$\delta_K = \int_0^1 e^{-2\pi i k \zeta} \sum_{n \in \mathbb{Z}} |\hat{f}(m + n)|^2 dm$$

This equation states that the function $F(m) = \sum_{n \in \mathbb{Z}} |\hat{f}(m + n)|^2$ with a period of one as a K^{th} Fourier coefficient equal to the Kronecker delta δ_K . It must therefore be equal to one almost everywhere. ■

3.2. Conjugate Mirror Filters

Lemma 13. (*Conjugate Mirror Filter*) Given an orthogonal MRA with a scaling function φ and a corresponding low-pass filter H , where $H(\zeta)$ is assumed to be a trigonometric polynomial with period one, the low-pass filter satisfies for almost every ζ .

$$|H(\zeta)|^2 + |H(\zeta + 1/2)|^2 = 1 \tag{22}$$

CHAPTER 3 SCALING EQUATION AND CONJUGATE MIRROR
CONDITIONS

$$H(\bar{z})\overline{H(\bar{z})} + H(\bar{z} + 1/2)\overline{H(\bar{z} + 1/2)} = 1$$

Proof 14. [13] Since the scaling function is assumed to be an orthonormal basis and the Fourier transform preserves orthonormality the integer translates of $\hat{\varphi}(\bar{z})$ will satisfy lemma 34. Thus we have

$$\sum_{n \in \mathbb{Z}} |\hat{\varphi}(\bar{z} + n)|^2 = 1 \quad (23)$$

Plugging equation (20) into (23) we obtain

$$1 = \sum_{n \in \mathbb{Z}} |\hat{\varphi}(\bar{z} + n)|^2 = \sum_{n \in \mathbb{Z}} \left| H\left(\frac{\bar{z} + n}{2}\right) \right|^2 \hat{\varphi} \left| \left(\frac{\bar{z} + n}{2}\right) \right|^2 \quad (24)$$

Then we will separate the sum over the odd and even integers. It follows,

$$\begin{aligned} & \sum_{n \in \mathbb{Z}} \left| H\left(\frac{\bar{z} + n}{2}\right) \right|^2 \hat{\varphi} \left| \left(\frac{\bar{z} + n}{2}\right) \right|^2 \\ &= \sum_{n \in \mathbb{Z}} \left| H\left(\frac{\bar{z} + 2n}{2}\right) \right|^2 \hat{\varphi} \left| \left(\frac{\bar{z} + 2n}{2}\right) \right|^2 \\ &+ \sum_{n \in \mathbb{Z}} \left| H\left(\frac{\bar{z} + 2n + 1}{2}\right) \right|^2 \hat{\varphi} \left| \left(\frac{\bar{z} + 2n + 1}{2}\right) \right|^2 = 1 \end{aligned}$$

Next we will use the fact that the function $H(\bar{z})$ has period one and factor it out of the integral and obtain

$$\left| H\left(\frac{\bar{z}}{2}\right) \right|^2 \sum_{n \in \mathbb{Z}} \hat{\varphi} \left| \left(\frac{\bar{z}}{2} + n\right) \right|^2 + \left| H\left(\frac{\bar{z}}{2} + \frac{1}{2}\right) \right|^2 \sum_{n \in \mathbb{Z}} \hat{\varphi} \left| \left(\frac{\bar{z}}{2} + n + \frac{1}{2}\right) \right|^2 = 1$$

CHAPTER 3 SCALING EQUATION AND CONJUGATE MIRROR CONDITIONS

Then we can once again use equation (23) since it is true almost everywhere by substitution we will arrive at

$$\left|H\left(\frac{z}{2}\right)\right|^2 + \left|H\left(\frac{z}{2} + \frac{1}{2}\right)\right|^2 = 1$$

Finally we may conclude that the equality of the above equation holds everywhere since $H(z)$ is a trigonometric polynomial by (Lemma 13) and is therefore continuous. Hence,

$$H(z)\overline{H(z)} + H\left(z + \frac{1}{2}\right)\overline{H\left(z + \frac{1}{2}\right)} = 1$$

■

3.3. The Wavelet and Conjugate Mirror Filters

We saw in (12) the projection of f onto the orthogonal space W_j was given by

$$Q_j f(t) = \sum_{k \in \mathbb{Z}} \langle f, \psi_{j,k} \rangle \psi_{j,k}(t)$$

where we defined $\psi_{j,k}$ by (8).

Theorem 15. ([13], Theorem 7.3) $\psi \in W_0 \subset V_{-1}$ we may express ψ as a superposition of $\varphi_{-1,k}$ where $\varphi_{-1,k}(t)$ forms an orthonormal basis of V_{-1} Meaning, there exists a sequence of coefficients $\{g_k\}_{k \in \mathbb{Z}}$ that satisfy the following scaling equation.

CHAPTER 3 SCALING EQUATION AND CONJUGATE MIRROR
CONDITIONS

$$\psi(t) = \sqrt{2} \sum_{k \in \mathbb{Z}} g_k \varphi(2t - k) \quad (25)$$

with the unique sequence of coefficients $\{g_k\}_{k \in \mathbb{Z}}$ known as the *high-pass filter*.

Theorem 16. [Meyer], [13] Let φ be a scaling function and $\{h\}_{k \in \mathbb{Z}}$ the corresponding conjugate mirror filter. Then on the Fourier side, (25) yields

$$\hat{\psi}(z) = G(z/2)\hat{\varphi}(z/2) \quad (26)$$

with $G(z)$ a trigonometric polynomial whose period is one and is given by its refinement mask

$$G(z) = \frac{1}{\sqrt{2}} \sum_{k \in \mathbb{Z}} g_k e^{-2\pi i k z} \quad (27)$$

where g_k is the *high-pass filter* defined by taking the inverse Fourier transform of (26)

$$g_k = (-1)^{1-k} h(1 - k) \quad (28)$$

Lemma 17. ([13], lemma 7.1) The family $\{\psi_{j,k}\}_{k \in \mathbb{Z}}$ is an orthonormal basis of W_j if and only if

$$|G(z)|^2 + |G(z + 1/2)|^2 = 1 \quad (29)$$

CHAPTER 3 SCALING EQUATION AND CONJUGATE MIRROR CONDITIONS

Proof 18. ([13], lemma 7.1) This proof follows much like proof 14. Plugging equation (26) into (21) we obtain

$$1 = \sum_{n \in \mathbb{Z}} |\widehat{\psi}(\frac{z}{2} + n)|^2 = \sum_{n \in \mathbb{Z}} \left| G\left(\frac{z}{2} + n\right) \right|^2 \widehat{\phi}\left(\frac{z}{2} + n\right) \right|^2 \quad (30)$$

Then we will separate the sum over the odd and even integers. It follows,

$$\begin{aligned} & \sum_{n \in \mathbb{Z}} \left| G\left(\frac{z}{2} + n\right) \right|^2 \widehat{\phi}\left(\frac{z}{2} + n\right) \right|^2 \\ &= \sum_{n \in \mathbb{Z}} \left| G\left(\frac{z}{2} + 2n\right) \right|^2 \widehat{\phi}\left(\frac{z}{2} + 2n\right) \right|^2 \\ &+ \sum_{n \in \mathbb{Z}} \left| G\left(\frac{z}{2} + 2n + 1\right) \right|^2 \widehat{\phi}\left(\frac{z}{2} + 2n + 1\right) \right|^2 = 1 \end{aligned}$$

Next we will use the fact that the function $G(z)$ has period one and factor it out of the integral and obtain

$$\left| G\left(\frac{z}{2}\right) \right|^2 \sum_{n \in \mathbb{Z}} \widehat{\phi}\left(\frac{z}{2} + n\right) \right|^2 + \left| G\left(\frac{z}{2} + \frac{1}{2}\right) \right|^2 \sum_{n \in \mathbb{Z}} \widehat{\phi}\left(\frac{z}{2} + n + \frac{1}{2}\right) \right|^2 = 1$$

Then we can once again use equation (23) by substitution we will arrive at

$$\left| G\left(\frac{z}{2}\right) \right|^2 + \left| G\left(\frac{z}{2} + \frac{1}{2}\right) \right|^2 = 1$$

Which is true everywhere since $G(z)$ is a trigonometric polynomial \

■

From the proof above we may conclude that $G(z)$ also satisfies a *conjugate mirror filter* condition and due to the orthogonality between W_0 and V_0 and our definition for $G(z)$ in (27) and (18) we have the following orthogonality condition on the level of the refinement masks

CHAPTER 3 SCALING EQUATION AND CONJUGATE MIRROR
CONDITIONS

$$|H(z)|\overline{|G(z)|} + |H(z + 1/2)|\overline{|G(z + 1/2)|} = 0 \quad (31)$$

Chapter 4 Biorthogonality and its Implication

In the previous chapters we introduced an orthogonal MRA and the associated scaling equations. We saw from Mallat's theorem that given an MRA with a scaling function we were guaranteed a wavelet that formed a basis for the orthogonal complement. As a consequence of the orthonormality of the scaling function we discovered conditions on the filter coefficients that insured reconstruction.

The use of FIRs made wavelets very computationally attractive. For example, given a finite signal of size N and an FIR with K non-zero entries, the fast wavelet transform can run on the order of $2KN$ [13]. As the application of wavelets progressed so too did the theory [7]. Practitioners continued to seek wavelets with different properties to solve new problems. These quests for different wavelets with unique properties began with the relaxing of the old. For instance in the following chapter we will discuss an alternative design to an MRA by removing the requirement of orthogonality between a scaling function and its wavelet and discusses the new biorthogonal conditions that insure perfect reconstruction.

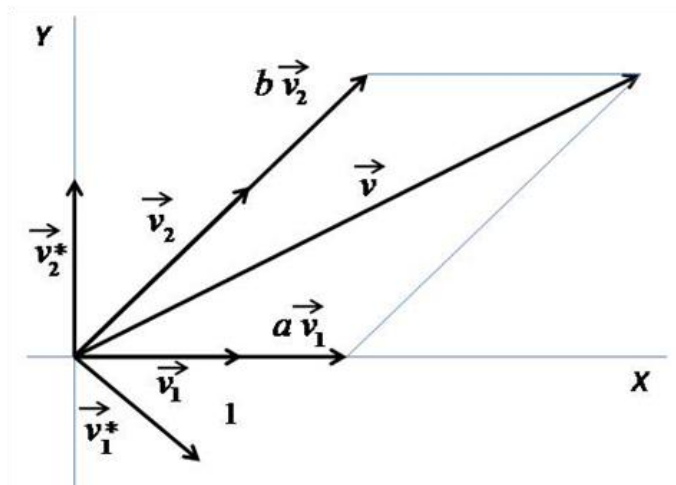


Figure 2. Biorthogonal Vectors in R^2

4.1. Biorthogonal MRA

Example 19. (Simple Biorthogonal Case) Consider the vectors $\vec{v}_1 = (1,0)$ and $\vec{v}_2 = (1,1)$ (Figure 2). We see that they are linearly independent but not orthogonal. These vectors will then form a basis for R^2 where $\forall \vec{v} = (x, y) \in R^2$ there exists unique coefficients a, b such that

$$\vec{v} = a\vec{v}_1 + b\vec{v}_2$$

In a biorthogonal case, there exist *dual vectors* \vec{v}_1^* and \vec{v}_2^* that allow us to take the inner products with these *dual vectors* to produce the coefficients a and b. These *dual vectors* satisfy (in our case) $\vec{v}_1^* \perp \vec{v}_2$ and $\vec{v}_2^* \perp \vec{v}_1$.

□

Our simple example above leads us to the definition of a biorthogonal basis.

Definition 20. ([7], **Biorthogonal basis**) For a Riesz basis $\{\psi_j\}_{j=1}^{\infty}$ the dual Riesz basis is a set of elements $\{\psi_k^*\}_{k=1}^{\infty}$ in a space \mathbf{H} such that $\langle \psi_j, \psi_k^* \rangle = \delta_{j,k}$ and any $f \in \mathbf{H}$ may be expressed as

$$f = \sum_{n=1}^{\infty} \langle f, \psi_n^* \rangle \psi_n = \sum_{n=1}^{\infty} \langle f, \psi_n \rangle \psi_n^*$$

A pair of dual Riesz bases $(\{\psi_j\}_{j=1}^{\infty}, \{\psi_k^*\}_{k=1}^{\infty})$ of \mathbf{H} will be referred to as a *biorthogonal basis*. For the definition of a Riesz bases please refer to the appendix.

Similar to our definition of an orthogonal MRA we also have properties that define a biorthogonal MRA. They are similar in that the scaling function defines the MRA. However we now have two dual scaling functions and no longer require orthogonality between a scaling function and its associated wavelet.

Definition 21. A *Biorthogonal Multiresolution Analysis* with scaling function φ and dual scaling function φ^* , satisfies the following properties

$$\forall j \in Z, V_{j+1} \subset V_j \text{ and } V_{j+1}^* \subset V_j^* \quad (32)$$

$$\forall j \in Z, f(t) \in V_j \Leftrightarrow f\left(\frac{t}{2}\right) \in V_{j+1} \text{ and} \quad (33)$$

$$f^*(t) \in V_j^* \Leftrightarrow f^*\left(\frac{t}{2}\right) \in V_{j+1}^*$$

$$\lim_{j \rightarrow +\infty} V_j = \bigcap_{j=-\infty}^{+\infty} V_j = \{0\} \text{ and} \quad (34)$$

$$\lim_{j \rightarrow +\infty} V_j^* = \bigcap_{j=-\infty}^{+\infty} V_j^* = \{0\}$$

$$\lim_{j \rightarrow -\infty} V_j = \text{closure} \left(\bigcup_{j=-\infty}^{j=+\infty} V_j \right) = L^2(R) \text{ and} \quad (35)$$

$$\lim_{j \rightarrow -\infty} V_j^* = \text{closure} \left(\bigcup_{j=-\infty}^{j=+\infty} V_j^* \right) = L^2(R)$$

The integer translates of φ and φ^* form a Riesz basis of V_0 and V_0^* respectively. (36)

CHAPTER 4 BIORTHOGONALITY AND ITS IMPLICATIONS

A biorthogonal MRA is very much like an orthogonal MRA in definition, the loss of orthogonality being the key difference. Simply, a biorthogonal MRA consists of two dual MRAs with two scaling functions φ and φ^* . The decomposition of the space $L^2(R)$ given by these two scaling functions is then

$$\dots V_3 \subset V_2 \subset V_1 \subset V_0 \subset V_{-1} \subset V_{-2} \subset V_{-3} \dots$$

and

$$\dots V_3^* \subset V_2^* \subset V_1^* \subset V_0^* \subset V_{-1}^* \subset V_{-2}^* \subset V_{-3}^* \dots$$

where by (34) the intersection of the spaces is the trivial space $\{0\}$ and by property (35) the union of the spaces is dense.

From property (36) the scaling function $\{\varphi_{j,k}\}_{k \in \mathbb{Z}}$ is a Riesz basis for V_j and $\{\varphi_{j,k}^*\}_{k \in \mathbb{Z}}$ is a Riesz basis for V_j^* ([13], [7]). For a definition of Riesz basis refer to the appendix Definition 7A and Definition 8A. We also require that these scaling functions be dual in the sense that

$$\langle \varphi_n, \varphi_j^* \rangle = \delta_{n,j}$$

Then for $f \in V_0$,

$$f(t) = \sum_{k \in \mathbb{Z}} \langle f, \varphi_{0,k}^* \rangle \varphi_{0,k}(t)$$

and if $f^* \in V_0^*$,

$$f^*(t) = \sum_{k \in \mathbb{Z}} \langle f^*, \varphi_{0,k} \rangle \varphi_{0,k}^*(t)$$

And just like an orthogonal MRA we can use the scaling functions to traverse across scales. This is seen in property (32 and 33).

Unlike an orthogonal MRA, the spaces V_j and W_j are no longer orthogonal (also true for the spaces V_j^* and W_j^*). We still relate the spaces by

$$V_j = V_{j+1} \oplus W_{j+1}$$

and

$$V_j^* = V_{j+1}^* \oplus W_{j+1}^*$$

only this time we impose the following conditions

$$V_j \perp W_j^* \text{ and } V_j^* \perp W_j$$

Where $\{\psi_{j,k}\}_{k \in \mathbb{Z}}$ and $\{\psi_{j,k}^*\}_{k \in \mathbb{Z}}$ are dual bases for W_j and W_j^* , respectively.

4.2. Biorthogonal Scaling equations

For a biorthogonal MRA the basic scaling equations (from [13]) are

$$\varphi(t) = \sqrt{2} \sum_{k \in \mathbb{Z}} h_k \varphi(2t - k) \text{ and } \varphi^*(t) = \sqrt{2} \sum_{k \in \mathbb{Z}} h_k^* \varphi^*(2t - k) \quad (37)$$

$$\psi(t) = \sqrt{2} \sum_{k \in \mathbb{Z}} g_k \psi(2t - k) \text{ and } \psi^*(t) = \sqrt{2} \sum_{k \in \mathbb{Z}} g_k^* \psi^*(2t - k) \quad (38)$$

And on the Fourier side, these equations become

$$\hat{\varphi}(\xi) = H(\xi/2) \hat{\varphi}(\xi/2) \text{ and } \hat{\varphi}^*(\xi) = H^*(\xi/2) \hat{\varphi}^*(\xi/2) \quad (39)$$

$$\hat{\psi}(\xi) = G(\xi/2) \hat{\psi}(\xi/2) \text{ and } \hat{\psi}^*(\xi) = G^*(\xi/2) \hat{\psi}^*(\xi/2) \quad (40)$$

Similar to what we observed in the orthogonal case, the scaling equations (37) and (38) in the biorthogonal MRA are defined implicitly from the dual scaling functions.

4.3. Finite Impulse Response Filters and the Fast Wavelet Transform

From (39) we can define the set of four FIR. With their refinement mask and using “z” notation we have

$$H(z) = \frac{1}{\sqrt{2}} \sum_{k \in \mathbb{Z}} h_k z^k \text{ and } H^*(z) = \frac{1}{\sqrt{2}} \sum_{k \in \mathbb{Z}} h_k^* z^k \quad (41)$$

with

$$G(z) = \overline{zH^*(z)} \text{ and } G^*(z) = \overline{zH(-z)} \quad (42)$$

and due to the biorthogonality we will have the following conditions

$$H(z)\overline{H^*(z)} + H(-z)\overline{H^*(-z)} = 1 \quad (43)$$

$$G(z)\overline{G^*(z)} + G(-z)\overline{G^*(-z)} = 1 \quad (44)$$

$$H(z)\overline{G^*(z)} + H(-z)\overline{G^*(-z)} = 0 \quad (45)$$

$$G(z)\overline{H^*(z)} + G(-z)\overline{H^*(-z)} = 0 \quad (46)$$

Decomposition

Synthesis

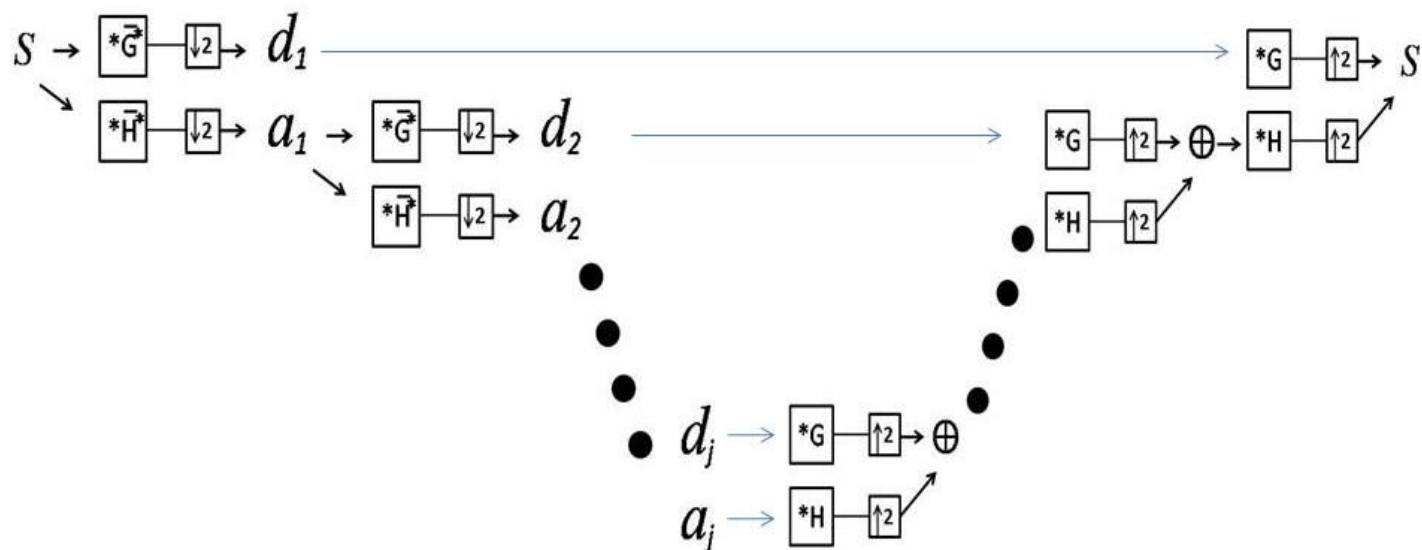


Figure 3 Biorthogonal Fast Wavelet Transform Schematic [9], [13]

Using the biorthogonal FIR (41,42) we may implement a fast wavelet transform for a signal S (Figure 3). On the side of decomposition the $*$ symbol is used to denote a convolution with the conjugate flip (denoted by a line over the filter) of the *high-pass filter* G^* and *low-pass filter* H^* and the $\downarrow 2$ is the down sampling operator where every even sample is removed. With the reconstruction or synthesis, the approximation and detail is convolved with the dual filters G and H . The $\uparrow 2$ is the up sampling operator adding in zeros in the even indices of the approximation or detail. The \oplus is the orthogonal summation.

Chapter 5 Wavelets and Electroencephalography

5.1. Background on Schizophrenia

Schizophrenia is a neurological disorder that influences behavior and cognitive function. It will often develop in young adults and is prevalent in approximately 1% of the general population. Thus, for the United States, nearly one million people suffer from Schizophrenia [ref needed]. Symptoms of Schizophrenia include hallucinations, delusions, inappropriate emotional responses, and paranoid behavior [ref needed]. For a review on Schizophrenia please refer to [ref needed].

While undeniably linked to genetics the mode of inheritance is unclear [ref need]. Having a relative with the condition is a strong risk factor for the disorder. However, diagnosing the condition is still a difficult task. The difficulty arises from the very thin boundaries between neurological disorders. It is not uncommon for a person diagnosed with schizophrenia to also suffer from other neurological disorders, such as bi-polar disorder [ref needed].

Electroencephalography (EEG) is a none-invasive tool that can be utilized to elucidate the mystery of schizophrenia. The goal is to execute wavelet analysis on EEG to decompose electrical potentials into exclusive time-frequency attributes. Studying the amplitudes and characteristics of these electrical potentials could potentially help diagnose patients and quantify cognitive impairment.

5.2. Materials and Methods

Data Collection

EEG from 116 participants was collected as part of a study conducted at the Hartford Hospital. The participants were either a healthy control group (HC group, N = 58) or a group of participants diagnosed with schizophrenic spectrum

CHAPTER 5 WAVELETS AND ELECTROENCEPHALOGRAPHY

psychological disorders (SZ group, $N = 58$). The standard 10-20 electrode placement was used with 64 Electrodes. The HC and SZ groups participated in a standard auditory oddball paradigm where they pressed a button when a target tone (1000 Hz) appeared within a series of standard auditory tones (1500 Hz). A total of 656 tones (20% targets) were presented to participants during the experiment. For more information on an auditory oddball paradigm please refer to [ref 1 and 15 in wikipedia].

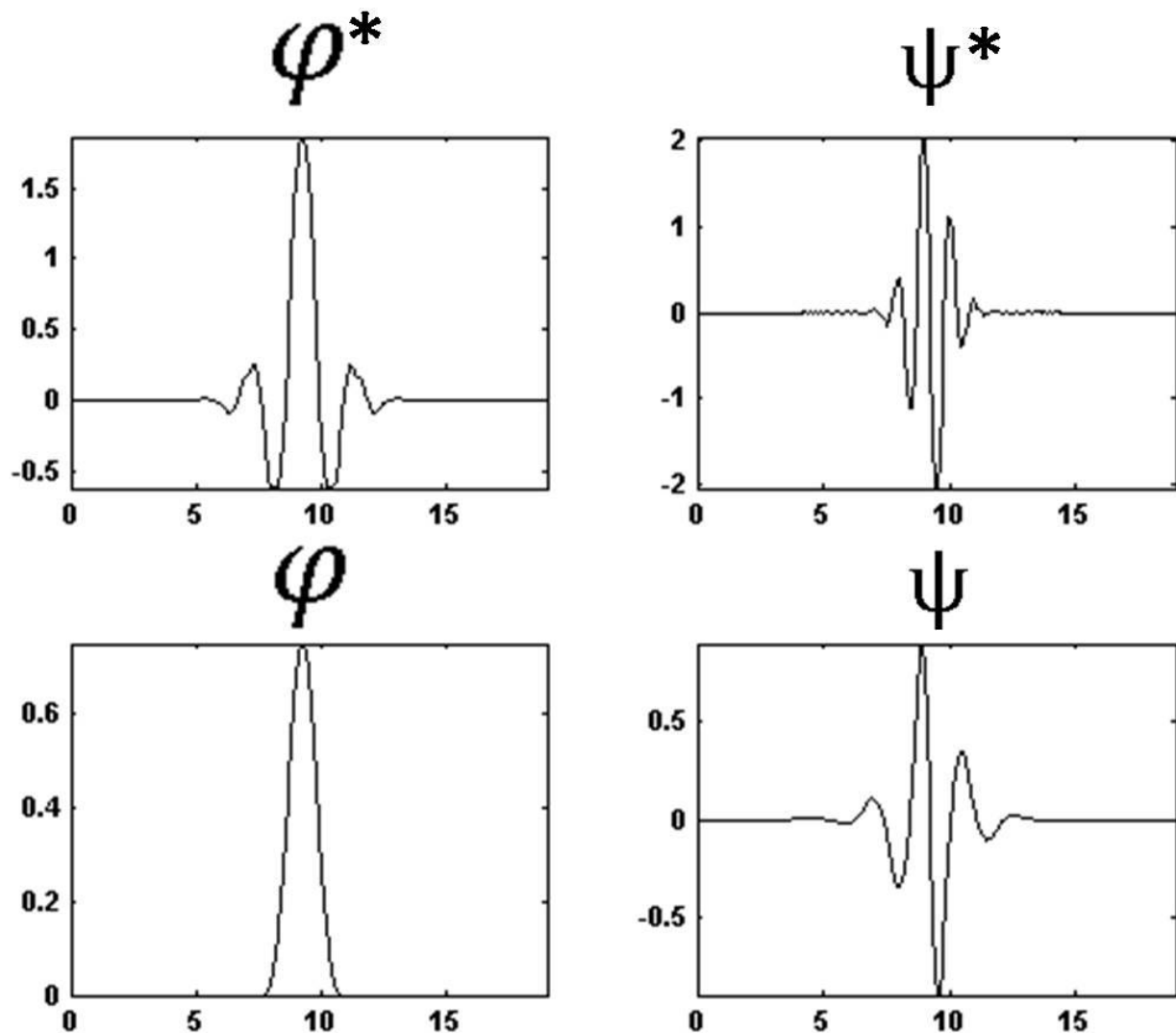


Figure 4. Dual Spline Scaling Functions and Biorthogonal Wavelets

De-noising and filtering

Independent component analysis was used to remove artifacts from the raw EEG. The biorthogonal spline wavelet (represented by the finite, bi-orthogonal, filter banks, see table above) was convolved with individual time series to calculate wavelet coefficients and to decompose the EEG into time-frequency representations. These time-frequency representations approximate the Hi-Gamma (65 – 125 Hz), gamma (32 – 65 Hz), Beta (16 – 32 Hz), alpha (8 – 16 Hz), theta (4 – 8 Hz), and delta (0-4 Hz) frequency bands. We focused analysis on the delta and theta frequency bands since they have the strongest contribution to the EEG response to targets [23].

$\overline{H_k^*}$	$\overline{G_k^*}$	H_k	G_k
-0.0007	0	0	-0.0007
0.0020	0	0	-0.0020
0.0051	0	0	0.0051
-0.0206	0	0	0.0206
-0.0141	0	0	-0.0141
0.0991	0	0	-0.0991
0.0123	0	0	0.0123
-0.3202	0	0	0.3202
0.0021	-0.1768	0.1768	0.0021
0.9421	0.5303	0.5303	-0.9421
0.9421	-0.5303	0.5303	0.9421
0.0021	0.1768	0.1768	-0.0021
-0.3202	0	0	-0.3202
0.0123	0	0	-0.0123
0.0991	0	0	0.0991
-0.0141	0	0	0.0141
-0.0206	0	0	-0.0206
0.0051	0	0	-0.0051
0.0020	0	0	0.0020
-0.0007	0	0	0.0007

Table 1 Biorthogonal Spline Finite Impulse Response Filter Banks

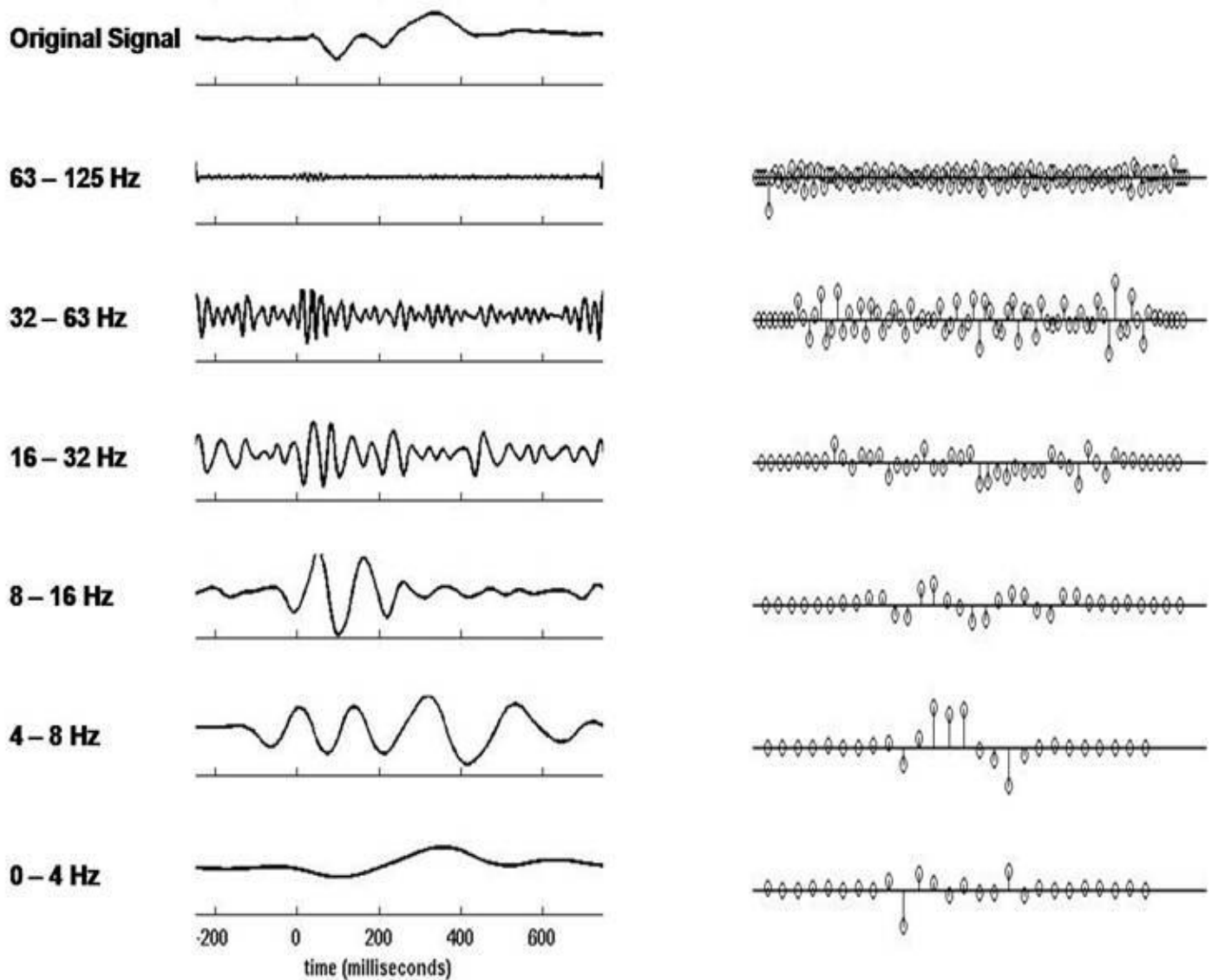


Figure 5 Single Sweep ERP Time-Frequency Representations and Wavelet Coefficients

Comparative wavelet analysis

Individual trials were decomposed using the fast biorthogonal wavelet transform with the dual scaling functions Φ and Φ^* and dual wavelets Ψ and Ψ^* (see figure 323). The wavelet coefficients were averaged separately for the 5 octaves and residual space (see figure 324) for target and non-target EEG segments. This was done for channels Fz, Cz, and Pz. A two-way-ANOVA was conducted separately for each octave and residual space, and channel, in order to examine the interaction between group (HC and SZ) and stimulus type (target or

CHAPTER 5 WAVELETS AND ELECTROENCEPHALOGRAPHY

non-target) for each coefficient and electrode. The coefficient and electrode with the smallest p-value was used as a feature in the subsequent analysis.

5.3. Results

Using the wavelet transform, the coefficients for responses were calculated for the HC and SZ groups. The 14th coefficient (which lies in the delta residual band (0-4Hz)) within channel Pz, demonstrates the strongest significant interaction between group (HC and SZ) and stimulus type (target or non-target) (see table 2).

Table 2 Two-Way-ANOVA of Channel Pz for 14th Delta (0 – 4 Hz) Coefficient

Channel Pz					
Source	Sum Sq.	d.f.	Mean Sq.	F	Prob>F
Subject	1786.4	1	1786.4	21.91	0
Targetness	12481.6	1	12481.6	153.1	0
Subject * Targetness	1119	1	1119	13.73	.0003
Error	18587.9	228	81.5		
Total	33974.9	231			

For the channel Pz using the Fast Wavelet Transform, individual responses were reconstructed and averaged separately for targets and non-targets. The P300 response (see Figure 6) was larger within the HC group (solid, red) compared to the SZ group (solid, green). This is consistent with previous research examining differences in P300 responses between the two groups [ref].

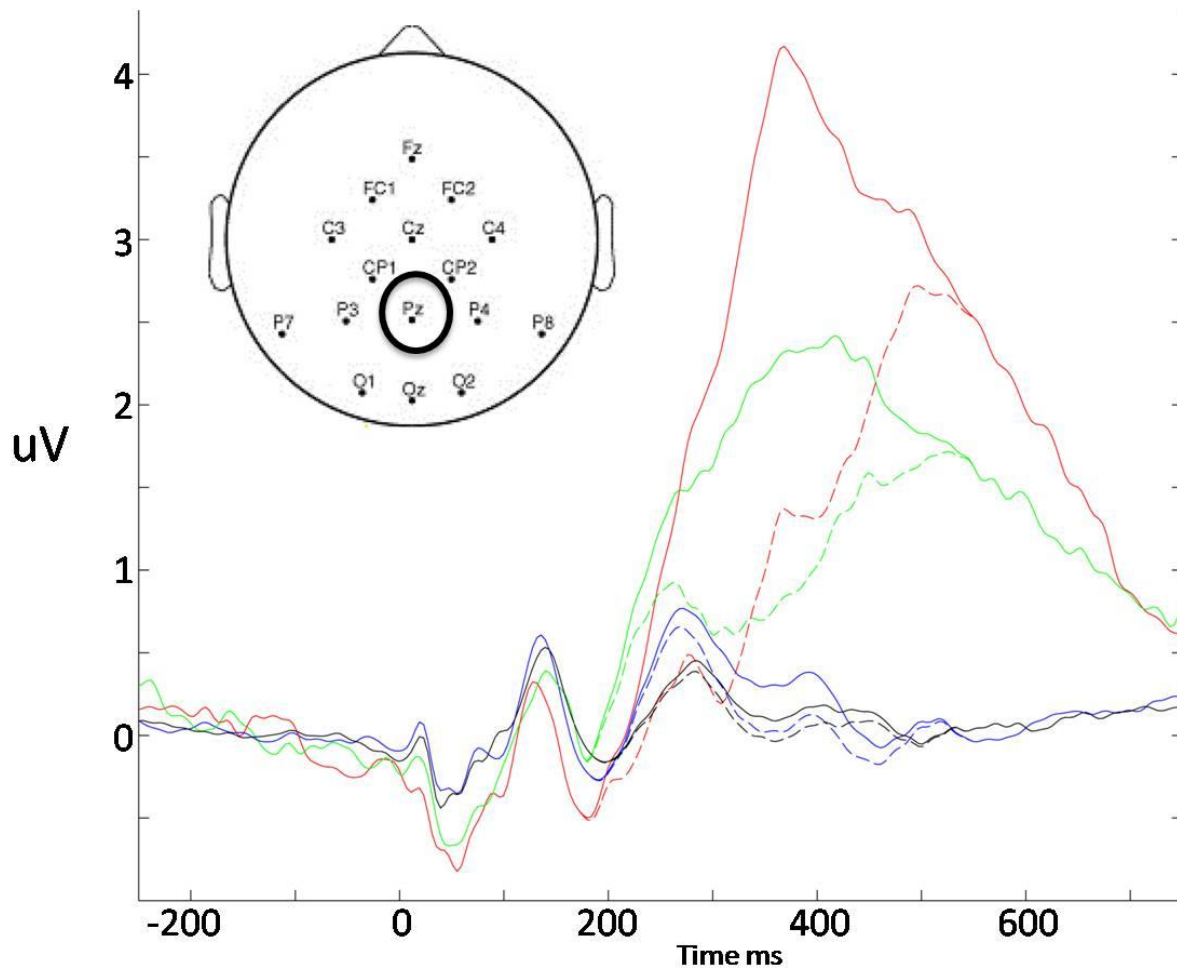


Figure 6 P300 ERP in micro volts (uV) for channel Pz

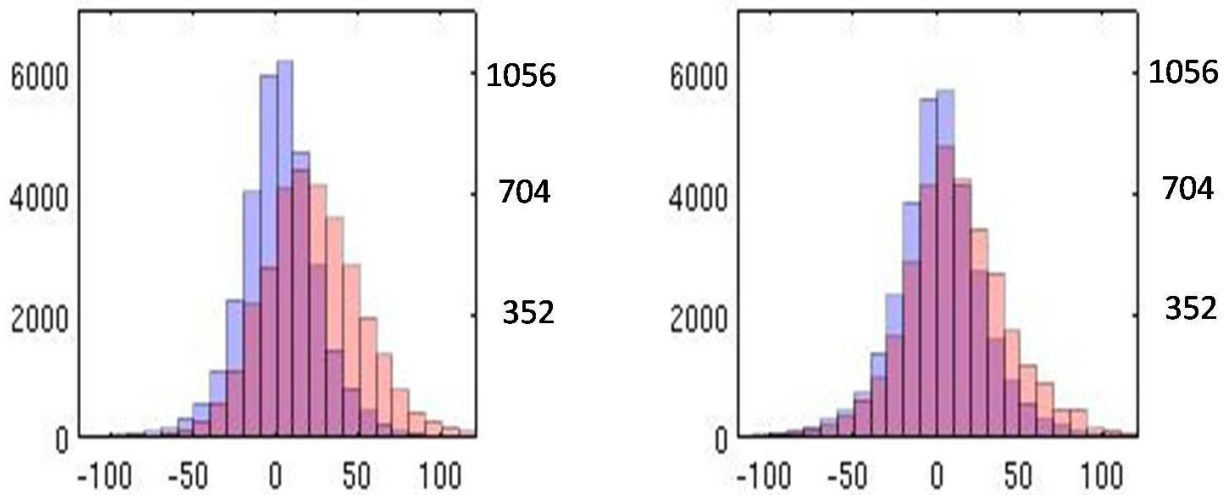


Figure 7 Histogram of 14th delta coefficient values (non-target response blue series, target responses orange series) for HC group (left) and SZ group (right).

Figure 7 demonstrates the distribution of values for channel Pz of the for 14th delta coefficient for each individual target and non-target trial. The vertical axis on the left of each histogram corresponds to the frequency of the “non-target” delta 14th coefficients, shown in blue bars. The axis on the right of each histogram corresponds to the frequency of the “target” delta 14th coefficients, shown in orange bars (the pink is the overlap between the two tones).

For the HC group (Figure 7, left) we saw that 76% of the responses to “target-tones” had a 14th delta coefficient above zero (orange series) and 54% of the responses to “non-target-tones” had a 14th delta-coefficient above zero (blue series). This observation was consistent with previous studies ([ref needed],[ref needed], [ref needed]).

In the SZ group (Figure 7, right) we saw that 64% of the response to “target-tones” had a 14th delta-coefficient above zero (orange series) and 52% of the responses to “non-target-tones” had a 14th delta coefficient above zero (blue series). We observed more separation of the 14th delta coefficient values between “target” and “non-target” tones within the HC group.

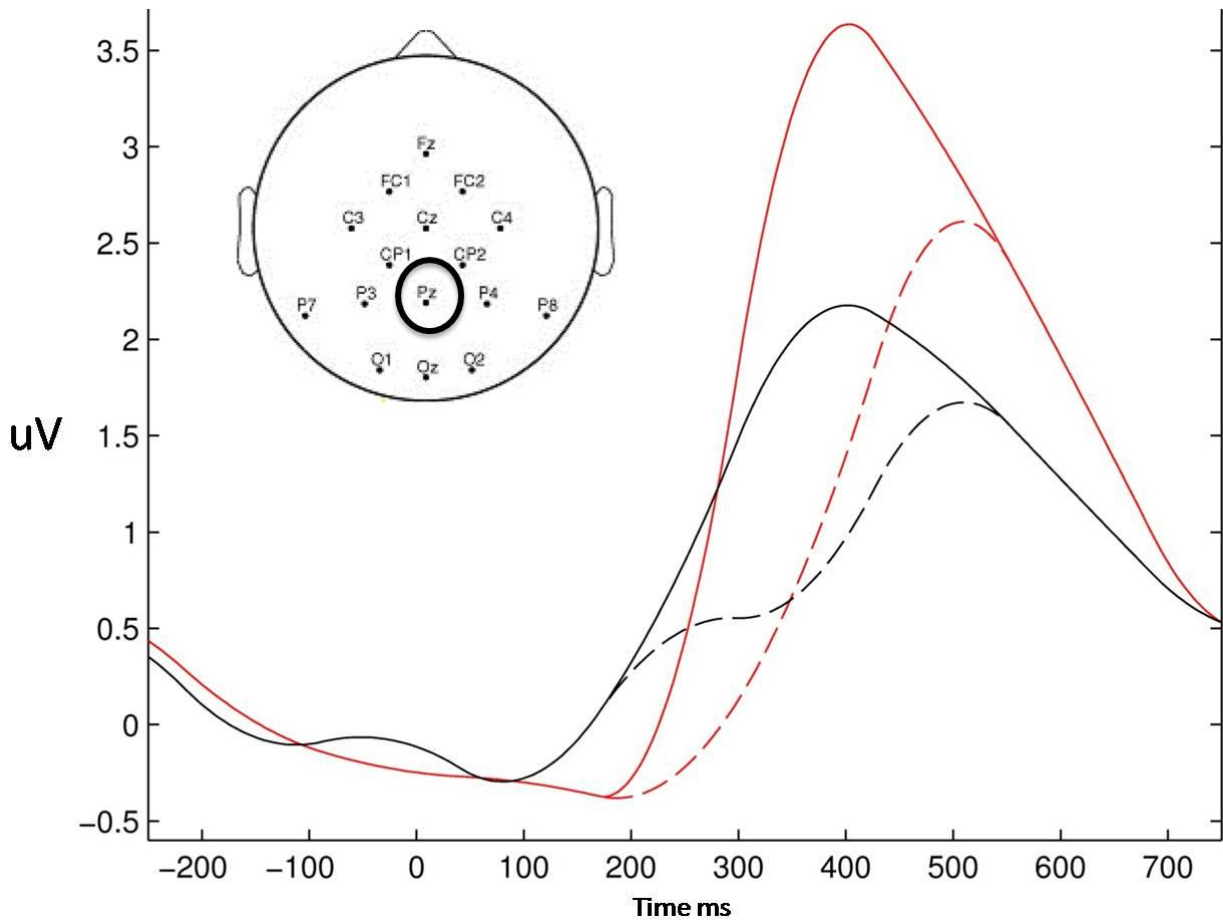


Figure 8 Delta (0 – 4 Hz) time-frequency representation for P300 ERP (channel Pz).

We additionally examined how the 14th delta coefficient contributed to the overall average ERP response. Responses were reconstructed for targets and non-targets with all coefficients and with the 14th coefficient set to zero. The P300 response was diminished when the 14th coefficient was removed, suggesting that it captures the main features of that ERP response.

5.4. Conclusions and Closing Remarks

The wavelet transform is a powerful tool for exploring EEG. When compared to other methods of analysis, the fast wavelet transform has several advantages. The first advantage being a part of its name; the fast wavelet transform is fast. For instance, the circular convolution of a finite signal of size N with an FIR containing at most K non-zero entries takes (at most) $2KN$ multiplications [ref needed (Mallat)]. Compared to the fast Fourier transform, which can be manipulated to run on the order of $N\log N$, if $2K < \log N$ then we see that the fast wavelet transform is quite fast!

Also, the ability to choose a wavelet with specific shape to use in analysis provides another unique advantage. When we use a biorthogonal spline wavelet we utilize the shape of the wavelet to extract the morphology of the P300 ERP. We are able to draw out P300 characteristics from the signal that would otherwise be lost when simply de-noising the signal with a high band pass filter [ref needed].

Furthermore the multiresolution property of the wavelet analysis generates time-frequency representations which not only provide information in the time domain, but also information regarding frequency. At distinct levels of frequency we utilized the approximation and details to observe how the signal is changing within a selected octave spaces. This allows us to reconstruct a signal utilizing preferred representations to generate a new signal at certain frequencies. We utilized this ability to reconstruct our ERP for the Delta (0 – 4 Hz) frequency range.

Additionally, we took advantage of the unique wavelet coefficients generated by the wavelet transform. Using these coefficients we identified a coefficient that differentiated our HC group from our SZ group. For this coefficient we saw a difference in the distribution of values for target responses between our HC group and SZ group. For our HC group we reproduced results from previous studies and discovered diminished results for our SZ group.

Appendix

Definition 1A (L^2 square itegrable functions). The space of square-itegrable functions

$$L^2(\mathbb{R}) := f: \mathbb{R} \rightarrow \mathbb{C} \text{ such that } \int_{\mathbb{R}} |f(t)|^2 dt < \infty$$

Definition 2A (Inner product). For V a vector space over \mathbb{R} (or \mathbb{C}), a function $\langle \cdot, \cdot \rangle : V \times V \rightarrow \mathbb{R}$ (or \mathbb{C}) is an inner product if:

- (1) For all $f \in V$, $\langle f, f \rangle \geq 0$ (positive);
- (2) $\langle f, f \rangle = 0$ if and on if $f = 0$ (positive definite);
- (3) for all $f, g, \in V$, $\langle f, g \rangle = \overline{\langle g, f \rangle}$ (hermitian):
- (4) for all $f, g, h \in V$ and $\alpha, \beta \in \mathbb{R}$ (or \mathbb{C}), $\langle \alpha f + \beta g, h \rangle = \alpha \langle f, h \rangle + \beta \langle g, h \rangle$ (linear).

Given an inner-product on V , we can define a norm by $\|f\|_{\mathbf{v}} = \sqrt{\langle f, f \rangle}$, called the norm induced by the inner product.

Definition 3A (L^2 inner product). The $L^2(\mathbb{R})$ inner product is defined by

$$\langle f, g \rangle = \int_{\mathbb{R}} f(t) \overline{g(t)} dt.$$

Definition 4A (L^2 norm induced by the inner product).

$$\|f\|_2 = \sqrt{\langle f, f \rangle} = \sqrt{\int_{\mathbb{R}} |f(t)|^2 dt}$$

Definition 5A (Orthonormal set). A set of elements $\{\psi_n\}$ in \mathbf{H} is orthonormal if their inner products obey

$$\langle \psi_n, \psi_m \rangle = \delta_{m,n},$$

where the Kronecker delta $\delta_{m,n}$ is defined by

$$\delta_{m,n} = \begin{cases} 1 & \text{if } m = n, \\ 0 & \text{if } m \neq n. \end{cases}$$

APPENDIX

Definition 6A (Orthonormal basis). The orthonormal set $\{\psi_n\}_{n=1}^{\infty}$ is an orthonormal basis if any $f \in \mathbf{H}$ can be reproduced as

$$f = \sum_{n=1}^{\infty} \langle f, \psi_n \rangle \psi_n,$$

with convergence in the norm of \mathbf{H} .

Definition 7A (Riesz basis). A set of elements $\{\psi_n\}_{n=1}^{\infty}$ in \mathbf{H} is a Riesz basis if it is a basis and there exist constants c and C with $0 < c \leq C < \infty$, such that for all $f \in \mathbf{H}$, the coefficients $\{\alpha_n = \alpha_n(f)\}_{n=1}^{\infty}$ satisfy

$$c \|f\|_{\mathbf{H}}^2 \leq \sum_{n=1}^{\infty} |\alpha_n|^2 \leq C \|f\|_{\mathbf{H}}^2.$$

Definition 8A (Dual Riesz basis and biorthogonal basis). For a Riesz basis, $\{\psi_n\}_{n=1}^{\infty}$, the dual Riesz basis is a set of elements $\{\psi_n^*\}_{n=1}^{\infty}$ in \mathbf{H} such that $\langle \psi_n, \psi_k^* \rangle = \delta_{n,k}$ (biorthogonality), and any $f \in \mathbf{H}$ can be expressed as

$$f = \sum_{n=1}^{\infty} \langle f, \psi_n^* \rangle \psi_n = \sum_{n=1}^{\infty} \langle f, \psi_n \rangle \psi_n^*.$$

with convergence in the norm of \mathbf{H} . We will call a pair of dual Riesz bases $(\{\psi_n\}_{n=1}^{\infty}, \{\psi_n^*\}_{n=1}^{\infty})$ in \mathbf{H} a biorthogonal basis.

Definition 9A (The Fourier transform). The *Fourier transform* \hat{f} of an itegrable function $f: \mathbb{R} \rightarrow \mathbb{R}$ is defined by:

$$\hat{f}(z) = \int_{\mathbb{R}} f(x) e^{-2\pi i z x} dx$$

Definition 10A (The inverse Fourier transform). The *inverse Fourier transform* $(g)\check{}$ of an itegrable function $g: \mathbb{R} \rightarrow \mathbb{R}$ is defined by:

$$(g)\check{(x)} = \int_{\mathbb{R}} g(z) e^{2\pi i z x} dz$$

BIBLIOGRAPHY

Bibliography

- [1.] Adelia, Hojjat, Zhou, Ziqin, and Dadmehr, Nahid. “Analysis of EEG records in an epileptic patient using wavelet transform.” *Journal of Neuroscience Methods* 123 (2003): 69-87. Print.
- [2.] Ademoglu,Ahmet, Micheli-Tzanakou,Evangelia, and Istefanopulos,Yorgo. “Analysis of Pattern Reversal Visual Evoked Potentials (PRVEP’s) by Spline Wavelets.” *EEE Transactions on Biomedical Engineering*, Vol. 44, No. 9, (1997): 881–890. Print.
- [3.] Barford, Lee A., R. Fazzio, Shane, and Smith, David R. Instruments and Photonics Laboratory. “An Introduction to Wavelets.” HPL-92-124, (September, 1992): 1–27.
- [4.] BasarErol, Demiralp Tamer, Schürmann Martin, Basar-ErogluCanan, and AdemogluAhmet. “Oscillatory Brain Dynamics, Wavelet Analysis, and Cognition.” *Brain and Language* 66, (1999): 146–183. Print.
- [5.] BasarErol, Schürmann, Martin, Demiralp, Tamer, Basar-Eroglu, Canan, and Ademoglu, Ahmet. “Event-related oscillations are ‘real brain responses’ — wavelet analysis and new strategies.” *International Journal of Psychophysiology* 39 (2001): 91–127. Print.
- [6.] Beck, Travis W., Housh, Terry J., Johnson Glen O., Weir, Joseph P., Cramer, Joel T., Coburn, Jared W., and Malek, Moh H. “Comparison of Fourier and wavelet transform procedures for examining the mechanomyographic and electromyographic frequency domain responses during fatiguing isokinetic muscle actions of the biceps brachii.” *Journal of Electromyography and Kinesiology* 15 (2005): 190–199. Print
- [7.] Daubechies, Ingrid. *Ten Lectures on Wavelets*. Montpelier, VT: Capital City Press (1994). Print.
- [8.] Demiralp, Tamer, Ademoglu, Ahmet, Schürmann, Martin, Basar-Eroglu, Canan, and Basar, Erol. “Detection of P300 Waves in Single Trials by the Wavelet Transform (WT).” *Brain and Language* 66, (1999): 108–128. Print.

BIBLIOGRAPHY

- [9.] Demiralp, Tamer, Yordanova, Juliana, Kolev, Vasil, Ademoglu, Ahmet, Devrim, Müge, and Samar, Vincent J. “Time–Frequency Analysis of Single-Sweep Event-Related Potentials by Means of Fast Wavelet Transform.” *Brain and Language* 66, (1999): 129–145. Print.
- [10.] Demiralpa, Tamer, Ademoglu, Ahmet, Istefanopulosb, Yorgo, Basar-Erogluc, Canan, and BasarErol. “Wavelet analysis of oddball P300.” *International Journal of Psychophysiology* 39 (2001): 221–227. Print.
- [11.] Hostens, I., Seghers, J., Spaepen, A., and Ramon, H. “Validation of the wavelet spectral estimation technique in Biceps Brachii and Brachioradialis fatigue assessment during prolonged low-level static and dynamic contractions.” *Journal of Electromyography and Kinesiology* 14 (2004): 205–215. Print.
- [12.] Kamont, Anna and Passenbrunner, Markus. “UNCONDITIONALITY OF ORTHOGONAL SPLIN SYSTEMS IN H^1 .” Cornell University arXiv:1404.5493 [math.FA], (2014). Print.
- [13.] Mallat,Stéphane, with contributions from Peyré, Gabriel. *A WAVELET TOUR OF SIGNAL PROCESSING*.Third edition. Burlington, MA: Academic Press (1999). Print.
- [14.] Mallat,Stephane, G., “MULTIRESOLUTION APPROXIMATIONS AND WAVELET ORTHONORMAL BASES OF $L^2(\mathbb{R})$.” *Transactions of the American Mathematical Society*. Volume 315, Number 1 (1989): 69–87. Print.
- [15.] Misiti, Michel, Misiti, Yves, Oppenheim, Georges, and Poggi, Jean-Michel. *Wavelet Toolbox for Use with MATLAB®*. Natick, MA: The MathWorks, Inc. (1996). Print.
- [16.] Mohlenkamp, Martin J. and Pereyra, María Christina. *Wavelets, Their Friends, and What They Can Do for You*. Edinburgh, U.K.: European Mathematical Society (2008). Print.

BIBLIOGRAPHY

- [17.] Pereyra, María Christina, and Lesley A. Ward. *Harmonic Analysis: From Fourier to Wavelets*. Providence, RI: American Mathematical Society, 2012. Print.
- [18.] Quiroga, Quian R. and Garcia, H. “Single-trial event-related potentials with wavelet denoising.” *Clinical Neurophysiology* 114 (2003): 376–390. Print.
- [19.] Quiroga, Quian R., Sakowitz, O.W., Basar, E., and Schürmann, M. “Wavelet Transform in the analysis of the frequency composition of evoked potentials.” *Brain Research Protocols* 8 (2001): 16–24. Print.
- [20.] Rosso, O.A., Martin, M.T., Figliola, A., Keller, K., and Plastino, A. “EEG analysis using wavelet-based information tools.” *Journal of Neuroscience Methods* 153 (2006): 163–182. Print.
- [21.] Samar, Vincent J. “Wavelet Analysis of Neuroelectric Waveforms.” *Brain and Language* 66, (1999): 1–6. Print.
- [22.] Samar, Vincent J. “Wavelet Analysis of Neuroelectric Waveforms: A Conceptual Tutorial.” *Brain and Language* 66, 7–60 (1999). Print.
- [23.] Demiralp, T. (1999) 'Detection of P300 waves in single trials by the wavelet transform (WT)', *Brain and Language*, vol. 66, pp. 108-128.
- [24.] Jeon, Y.W. (2003), 'Meta-analysis of P300 and schizophrenia: patients, paradigms, and practical implications', *Psychophysiology*, vol. 40, pp. 684-701.

Jung, T.-P., Makeig, S., Humphries, C., Lee, T.-W., Mckeown, M. J., Iragui, V., & Sejnowski, T. J. (2000). Removing electroencephalographic artifacts by blind source separation. *Psychophysiology*, 37(2), 163–178.